Iran Polym J (2015) 24:505–513
DOI 10.1007/s13726-015-0341-4

ORIGINAL PAPER

Effect of ionic group content on thermal and structural properties of polycaprolactone-based shape memory polyurethane ionomers

Milad Momtaz[1] · **Mehdi Barikani**[1] · **Mohammad Razavi-Nouri**[1]

Received: 9 September 2014 / Accepted: 28 April 2015 / Published online: 9 May 2015

Abstract In this work, the effect of ionic group content on thermal, structural, and shape memory properties of segmented polyurethane ionomers based on polycaprolactone diol, diphenylmethane diisocyanate, 1,4-butanediol, dimethylol propionic acid, and triethyl amine was investigated. Fourier transform infrared spectroscopy was used to check the accomplishment of the synthesis. Thermal, structural, and shape memory properties of the synthesized shape memory polyurethanes were measured using different techniques such as differential scanning calorimetry, thermogravimetric analysis (TGA), wide-angle X-ray diffraction, and tensile cyclic tests. It was found that the ionomers with higher amount of ionic groups have relatively stronger crystallization tendency. In addition, the glass transition temperature of soft segments was influenced by the degree of phase separation. It was observed that the degree of phase separation improved when the amount of ionization was higher than a critical value. The increased polarity difference of soft and hard phase upon ionization could be the driving force for increased phase separation. The results obtained from TGA showed that the thermal stability of the ionomers was lower than that of the non-ionomer sample. This can be attributed to the reduction of hydrogen bond formation and decrease of cohesion in the hard domains of ionomers. In addition, ionic group content affected the shape recovery of the material, where this parameter increased with the increase of ionic groups.

✉ Mehdi Barikani
m.barikani@ippi.ac.ir

[1] Iran Polymer and Petrochemical Institute,
P.O. Box 14965-115, Tehran, Iran

Keywords Polyurethane · Ionomer · Tensile cyclic test · Shape fixity · Shape recovery

Introduction

The distinct shape memory behavior in some materials such as polymers and alloys [1] has attracted a great attention worldwide. In recent years, shape memory polymers (SMPs) have been studied intensively in both academic and industrial sectors for their low cost, good processability, high recoverable strain, and larger range of shape recovery temperatures (R_r) in comparison with those parameters of shape memory alloys [2, 3]. A majority of SMPs have been stimulated by the application of heat [4]. However, cooling, water [5], and moisture-responsive [6] shape memory effects (SME) have been also reported. It has been stated that the thermo- and chemo-responsive SME are intrinsic properties of many synthetic and natural polymers. Based on this mechanism, new materials with tailored features could be designed [7].

Among the SMPs, segmented shape memory polyurethanes (SMPUs) are the thermoplastic block copolymers having the unique mechanical and shape memory properties [8, 9]. These polymers mainly consist of soft and hard domains, in which the former and latter constitute the reversible and frozen phase, respectively [10, 11]. The reversible phase is responsible for holding the temporary deformation. However, the frozen phase, which contains physical or chemical crosslink points, inhibits slip of the molecular chains and is responsible for memorizing the permanent shape [12, 13]. The SMPUs can memorize the permanent shape and recover from the temporary shape upon heating above a switching temperature (T_S) that could be the melting point (T_m) or glass transition temperature

(T_g) of the soft segments [14]. A polyurethane is called T_g—based SMPU if the soft domains use glass transition temperature as the switching temperature. T_m—based SMPUs, on the other hand, have gained much attention because the melting temperature of crystals is a sharper transition in comparison with the glass transition. This is a prerequisite for having good shape fixity (R_f).The strong intermolecular forces between the hard domains result from the hydrogen bonding and high polarity of the urethane and urea groups. Thus, the shape recovery of polyurethane is mainly influenced by the hard domains and the moiety of their molecular structure [15]. In addition, soft segment molecular weight and morphological structure both dominate the shape fixity of SMPUs [16, 17].

Ionomers are a group of functional polymers and their specific functions result from the existence of electrostatic interactions of the ionic groups. These polymers exhibit superior characteristics in comparison with non-ionomers, in which some physical properties such as fluidity at elevated temperatures, dynamic and adhesion properties are of high significance [18]. Polyurethane ionomers can also show superior mechanical properties in comparison with non-ionomers. Tensile strength, modulus, and elongation-at-break of polyurethane ionomers could be increased because of the presence of Columbic forces between the ionic groups within the polymer chains [19].

Hu et al. [20] studied the crystallization and melting behavior of soft segments in shape memory polyurethane ionomers based on polycaprolactone diols (PCL-diols), 4,4′-diphenylmethane diisocyanate (MDI), 1,4-butanediol (1,4-BDO), and *N*,*N*-bis (2-hydroxyethyl) isonicotinamide (BIN). They investigated the isothermal crystallization of SMPUs and found that the introduction of ionic groups into the hard segments not only decreased the rate of crystallization significantly, but also the increase of BIN content reduced crystallization, as well.

Zhu et al. [21] studied the effect of cationic group content on shape memory properties of polyurethanes containing PCL-diol, MDI, 1,4-BDO, BIN, and *N*-methyldiethanolamine (NMDA). They reported that cationic groups had a dominant effect on the shape fixity and recovery of NMDA series, whereas ionic groups had no effect on the shape memory properties of the samples containing BIN.

In this work, a series of polycaprolactone-based SMPU ionomers with different anionic group content were synthesized using polycaprolactone diol (PCL-diol), 4,4′-methylenediphenyl diisocyanate (MDI), 1,4-butanediol (1,4-BDO), 2,2-bis (hydroxyl methyl) propionic acid (DMPA), and triethyl amine (TEA) by bulk polymerization method. Fourier transform infrared (FTIR) spectroscopy was utilized to check the accomplishment of polyurethanes synthesis. Thermal and structural properties were evaluated using differential scanning calorimetry (DSC), thermogravimetric analysis (TGA), and wide-angle X-ray diffraction (WAXD) techniques. Shape memory properties were also studied by thermomechanical cyclic tests.

Experimental

Materials

Polycaprolactone diol with average molecular weight of 4000 (namely CAPA4000), which was dried at 80 °C under vacuum for 24 h before use, was supplied by Solvay Interox (UK). MDI was purchased from Aldrich (USA) and used to synthesize the samples without further treatment. DMF and 1,4-BDO were both supplied by Merck (Germany) and dried using proper molecular sieves for several days before use. DMPA was purchased from Aldrich (USA) and used as the second chain extender after drying at 80 °C under vacuum for 48 h. TEA was provided by Merck (Germany) and used without any further treatment.

Synthesis of SMPU ionomers

Five samples with various ionic group content were synthesized by the pre-polymerization method. A 500-mL, round-bottom, four-necked separable flask equipped with a mechanical stirrer, a thermometer, a condenser with a drying tube, and a nitrogen inlet was used as the reactor. The samples were synthesized by bulk polymerization in DMF as the solvent under dry N_2 in three steps. First, proper amounts of MDI and PCL-diol in 100 mL of DMF, which was freshly distilled before use, were stirred under nitrogen at 80 °C for 2 h to make the prepolymer. 1,4-BDO was added subsequently according to the MDI/PCL selected ratios and the reaction was continued for 30 min. Afterwards, DMPA dissolved in 10 mL of fresh DMF was added to the reactor and the reaction was continued at 50 °C for another 1 h. The main reason for the reduction of reactor temperature was to prevent the reaction of DMPA acidic group with isocyanate. Finally, the neutralization reaction was carried out by the addition of TEA to the reaction mixture and the reaction was continued at ambient temperature for another 30 min. The prepolymer preparation step, as well as chain extension and neutralization reaction, is shown in Scheme 1. After the polymerization, the samples were removed of air bubbles under vacuum and further solidified in an oven at 100 °C for 24 h [22]. The compositions of the prepared samples are shown in Table 1.

Characterization

A Bruker Equinox 55 FTIR (Germany) spectrometer was used to identify the formation of urethane linkages and

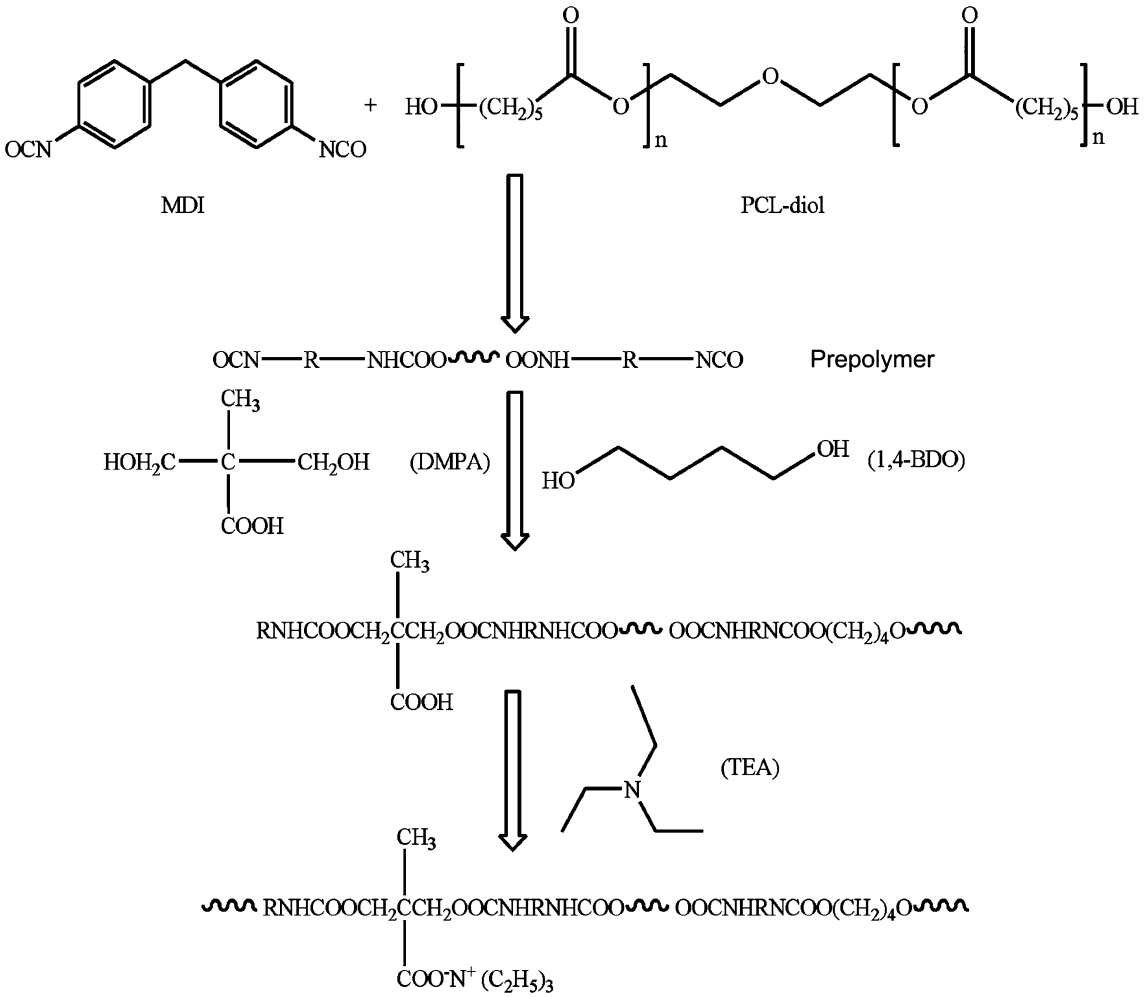

Scheme 1 The prepolymerization, chain extension, and neutralization reactions for the prepared polyurethane ionomers

Table 1 Composition of PCL-based SMPU samples

Sample name	SSL (g/mol)	HSC (%)	Molar ratios CAPA/MDI/1,4-BDO/DMPA/TEA	DMPA (wt%)	DMPA (mol %)
4000-24	4000	24	1/4/3/0/0	0	0
Ionomer I	4000	24	1/4/2.5/0.5/0.5	23	17
Ionomer II	4000	24	1/4/1.5/1.5/1.5	60	50
Ionomer III	4000	24	1/4/0.5/2.5/2.5	88	83
Ionomer IV	4000	24	1/4/0/3/3	100	100

further accomplishment of the synthesis. A Perkin-Elmer DSC instrument was used to study the thermal behavior of the samples, each weighing 5 ± 0.1 mg. Each sample was first heated up from −80 to 220 °C at a constant heating rate of 10 °C/min and held at 220 °C for 1 min; afterwards, the sample was cooled to −80 °C at a cooling rate of 10 °C/min, held at this temperature for another 1 min, and then reheated to 220 °C at the same heating rate. Thermogravimetric analysis (TGA) was used to study the thermal stability of the SMPUs. The TGA measurements were carried out in air with a heating rate of 5 °C/min using a Perkin-Elmer TGA instrument.

X-ray diffraction analysis was performed for all the samples right after their synthesis on a Siemens D5000 X-ray diffractometer using CuKα radiation ($\lambda = 1.54$ Å) at a scanning rate of 1°/min for all the specimens. An Instron 6022 apparatus equipped with a temperature-controlled chamber was utilized to perform the cyclic tensile tests.

Samples each having the dimensions of 20 × 2 × 0.5 mm were first heated up to the temperature of 70 °C (T_{high}) in 600 s. Every sample was then stretched to the maximum elongation (ε_m) of 50 % at a constant strain rate of 0.5 min^{-1} at T_{high}. While the sample was held at the same strain, nitrogen was purged into the chamber to reduce the temperature to −20 °C (T_{low}) to freeze the specimen. Afterwards, the strain was released to zero to let the sample relax and reheating began for another 600 s. The shape fixity [$R_f(N)$] and shape recovery [$R_r(N)$]after the Nth cycle were calculated by the following equations [23]:

$$R_f(N) = \frac{\varepsilon_u(N)}{\varepsilon_m} \quad (1)$$

$$R_r(N) = \frac{[\varepsilon_m - \varepsilon_p(N)]}{\varepsilon_m}, \quad (2)$$

where $\varepsilon_p(N)$ is the measured strain at the Nth cycle of the thermo-mechanical analysis, $\varepsilon_u(N)$ is the sample strain right after unloading at the Nth cycle, and ε_m is the maximum applied strain to the sample. Shape fixity represents sample's ability to keep its temporary shape and shape recovery shows the extent to which a sample retracts to its original shape.

Results and discussion

Spectroscopic characterization

FTIR spectra of all the samples are shown in Fig. 1. As it can be observed, the disappearing of the peak at 2270 cm^{-1}, which is the characteristic peak of the isocyanate group, and the existence of the two characteristic peaks of urethanes at 1720 and 3324 cm^{-1}, which are related to the stretching of C=O and –NH groups, respectively, imply that the synthesis of polyurethanes have been completed.

The peak at 3324 cm^{-1} has been broadened with the increase of DMPA content in the samples [24]. The peaks at 2930 and 2850 cm^{-1} belong to the asymmetric and symmetric stretching modes of methylene groups, respectively [25], which both have been intensified with the addition of DMPA in the ionomers [23, 26]. The peaks at 1530 and 1170 cm^{-1}, which are present at both ionomer and non-ionomer samples, correspond to the –NH bending and –C–O–C– stretching, respectively [27, 28]. The peak at 1720 cm^{-1} is attributed to the carbonyl groups, which is a sharp one in the spectrum of non-ionomer sample, but has been broadened for the ionomers [29]. This could be attributed to the simultaneous reactions of MDI with 1,4-BDO and DMPA, which result in the formation of more carbonyl groups [23, 30].

Formation of hydrogen bonding between carbonyl and –NH groups, as well as segmental polarity differences is

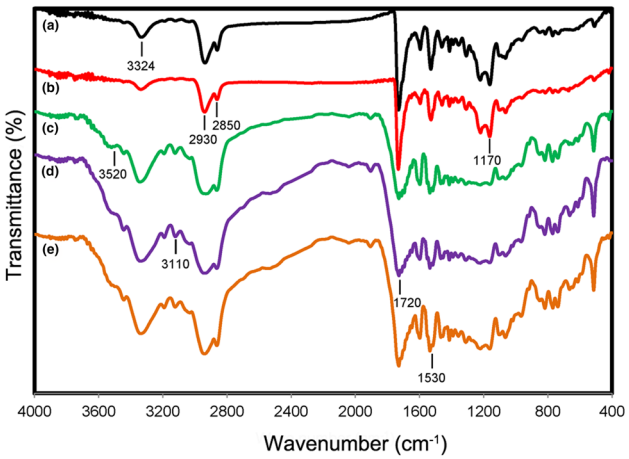

Fig. 1 Typical FTIR spectra of SMPUs: **a** 4000-24, **b** ionomer I, **c** ionomer II, **d** ionomer III and **e** ionomer IV samples

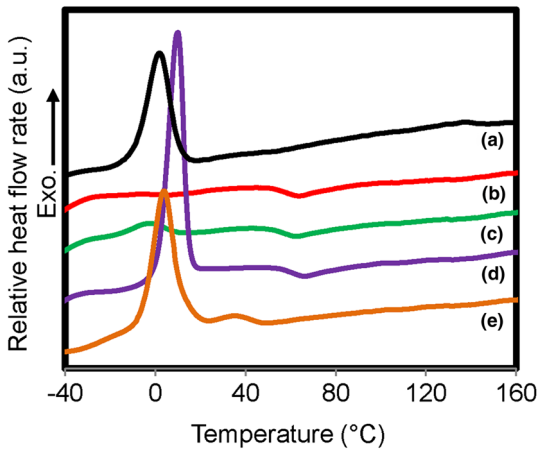

Fig. 2 DSC cooling scans of: **a** 4000-24, **b** ionomer I, **c** ionomer II, **d** ionomer III, and **e** ionomer IV samples

responsible for the separation of hard and soft phases [31, 32]. The degree of phase separation could partially be under the control of ionic group content [33, 34]. Incorporation of an asymmetrical diisocyanate and chain extender during synthesis disrupts the ordered hard domains probably [35], whereas a symmetrical chain extender can contrastingly increase the ordered hard domains leading to the formation of more phase-separated structures in the ionomers. The observed peaks of the ionomers at 3520 and 3110 cm^{-1} might be related to the –OH and –CH groups of DMPA, respectively.

Thermal analysis

The cooling and heating scans of the samples are shown in Figs. 2 and 3, respectively. The glass transition ($T_{g\cdot s}$), melting ($T_{m\cdot s}$), and crystallization temperatures ($T_{c\cdot s}$), as well as

the enthalpy of melting ($\Delta H_{m\cdot s}$) and crystallization of the soft segments ($\Delta H_{c\cdot s}$) and the degree of crystallization of soft segments ($X_{c\cdot s}$) are shown in Table 2. The degree of the crystallization of soft segments was calculated using the following equation:

$$X_{c\cdot s} = \frac{\Delta H_{m\cdot s}}{\Delta H_m^*} \times 100, \quad (3)$$

where ΔH_m^* is the melting enthalpy of the 100 % crystalline PCL-diol with the number average molecular weight of 4000 (142 J/g) [36]. As observed from Fig. 2, ionomer I shows no crystalline peak and ionomer II reveals a rather weak peak on cooling. This is probably because of the fact that the amount of Columbic forces in the ionic groups is not that much to assist the polymeric chains to be placed in crystalline phase. However, the soft segments of these two ionomers have the possibility to rearrange and reform to create the crystalline regions during heating, i.e., cold crystallization (Fig. 3). Unlike ionomers I and II, the three other samples showed no cold crystallization peaks at heating scans, implying their higher ability for crystallization on cooling.

Figure 2 also shows that crystallization can take place for the ionomers III and IV, which can be attributed to the higher amount of Columbic forces between the polymeric chains. Therefore, the crystallization tendency of the ionomers is improved with the increase of ionic group content.

The glass transition temperature of soft segments is influenced by the degree of phase separation in segmented polyurethanes. As the phase separation is decreased, $T_{g\cdot s}$ value will be increased [32, 37]. Figure 3 indicates that there is a baseline change for all the samples in the range −55 to −35 °C, which is related to $T_{g\cdot s}$ values. These values are shown in Table 2.

In constant hard segment content (HSC), increase in ionic group content resulted in more Columbic forces in the hard domains due to the presence of ionic interactions between TEA and DMPA. As a result, the mobility of polymeric chains in soft domains is limited and $T_{g\cdot s}$ of samples will be increased. The increase in $T_{g\cdot s}$ values from 4000-24 to ionomer III is probably due to the disruption of hard segments ordering and their solubilization in the soft phase, leading to the formation of more mixed phases. Introduction of ionic groups into the hard segments has two contrasting effects. On one hand, the ordered structure of hard domains was disrupted. On the other hand, the increase of ionic groups resulted in the formation of more Columbic forces between these groups. Further ionization, from ionomer III to IV, causes a decrease in $T_{g\cdot s}$ values, indicating an increase in phase separation. The phase-separation driving force could be attributed to the increased polarity difference of the two phases upon ionization. It could be concluded that this difference overcomes the hard segment packing arrangements [38].

It was observed that the melting temperature of soft segments enhanced slightly; however, the enthalpy of melting increased significantly with the increase of ionic group content, implying that the introduction of ionic groups improved the degree of crystallinity of soft segments. The crystallinity of soft segments was increased up to the ionomer III, but reduced for the ionomer IV. This could be attributed to the fact that probably with the increase of Columbic forces from a critical value, hard segments constitute a strong framework by which the soft segment crystallinity is enormously affected. Unlike the soft segments, there was no melting peak for the hard domains that could be related to the existence of low hard segment content [20]. Cooling and heating scans revealed that ionomers with higher amount of ionic groups have relatively stronger

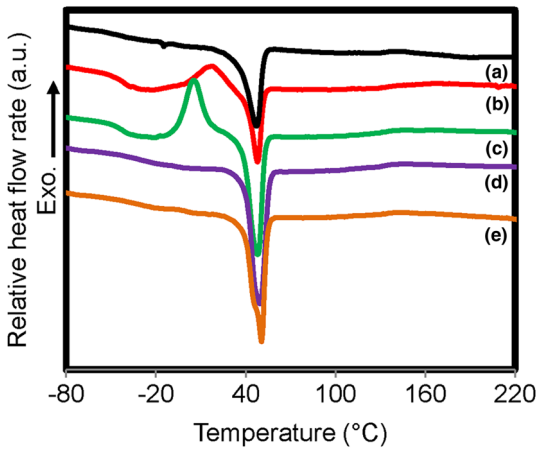

Fig. 3 DSC heating scans of: **a** 4000-24, **b** ionomer I, **c** ionomer II, **d** ionomer III, and **e** ionomer IV samples

Table 2 Thermal properties of the prepared samples obtained from DSC

Sample name	$T_{g\cdot s}$ (°C)	$T_{m\cdot s}$ (°C)	$\Delta H_{m\cdot s}$ (J/g)	$X_{c\cdot s}$ (%)	$T_{c\cdot s}$ (°C)	$T_{c\cdot c\cdot s}$ (°C)	$\Delta H_{c\cdot s}$ (J/g)
4000-24	−53.9	47.7	28.8	20.3	1.6	–	29.4
Ionomer I	−47.5	47.9	31.5	22.2	–	18	–
Ionomer II	−45.8	47.8	41.6	29.3	5.3	5.3	–
Ionomer III	−32.8	50.0	52.0	36.6	9.3	–	51.7
Ionomer IV	−37.2	49.9	44.5	31.3	3.4	–	54.7

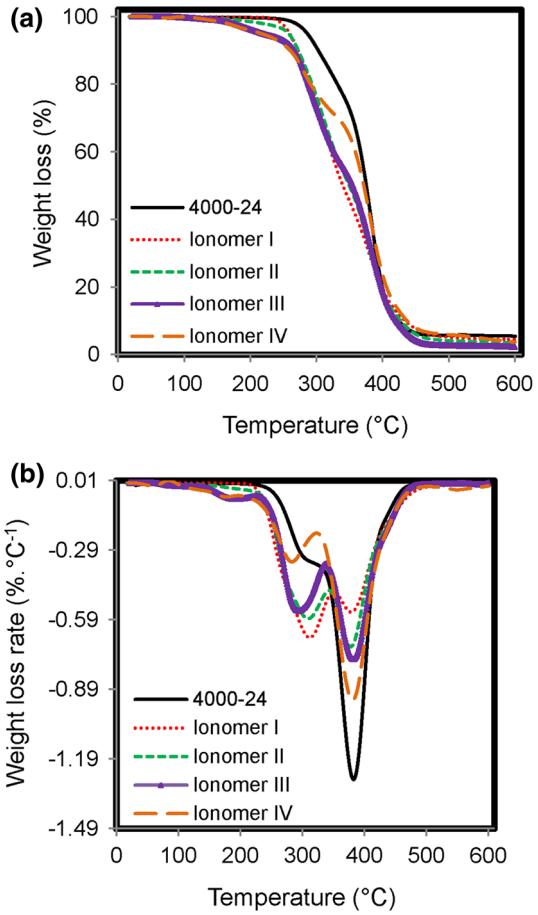

Fig. 4 Thermogravimetric curves of the samples: **a** variation of weight loss and **b** weight loss rate with temperature

Table 3 Thermogravimetric data of the prepared samples

Sample name	T_{onset} (°C)	$T_{D\cdot1}$ (°C)	$T_{D\cdot2}$ (°C)
4000-24	286	297	383
Ionomer I	259	312	381
Ionomer II	257	310	383
Ionomer III	217	293	379
Ionomer IV	215	283	380

crystallization tendency. Furthermore, the degree of phase separation was influenced by the amount of ionization, which has appeared in $T_{g\cdot s}$ values.

Thermal degradation studies give a chance to choose appropriate conditions for processing, manipulating, and obtaining high-quality products. In addition, TGA is a proper method for calculating the lifetime of materials [39]. Thermogravimetric analysis was performed to draw a comparison between the thermal stability of the samples, which is shown in Fig. 4a, b. The data obtained from these analyses are also presented in Table 3. The data indicate that the temperatures at five percent weight loss (T_{onset}) of 4000-24 sample was higher than that of the ionomers; therefore, it can be concluded that the increase of ionic group content decreased the thermal stability of the samples.

As illustrated in Fig. 4b, two peaks which represent the maximum rate of degradation are observed for all the studied samples. The first peak of degradation, which starts at the temperature ($T_{D\cdot1}$) range of 220–230 °C, is attributed to the thermal degradation of urethane groups in hard segments [26, 40]. Accordingly, by adding ionic groups to 4000-24, the first peak was enlarged. This could be due to the fact that the incorporation of ionic moieties to the hard segments reduced the cohesion of hydrogen bonds and thus, the degradation rate was enhanced.

By increasing ionic groups, the first peak was also shifted to the lower temperatures. This is primarily because of the decarboxylation of DMPA and formation of more thermodynamically stable carbon dioxide and alkene molecules. Secondarily, the steric hindrance of bulky acid groups in the hard domains inhibits the formation of hydrogen bonds via urethane interactions. As a result, the cohesion of hard segments is reduced and less thermal energy would be sufficient to overcome this physical barrier. Therefore, as the temperature was increased, this energy is used for the initiation of degradation of chemical bonds in polymeric chains. The second peak of degradation, which was observed at much higher temperatures ($T_{D\cdot2}$), could be attributed to the thermal degradation of polyesters. This indicates that polyesters are more thermally stable than urethane groups. In general, the thermal stability of the samples was deteriorated with the increase of ionic group content.

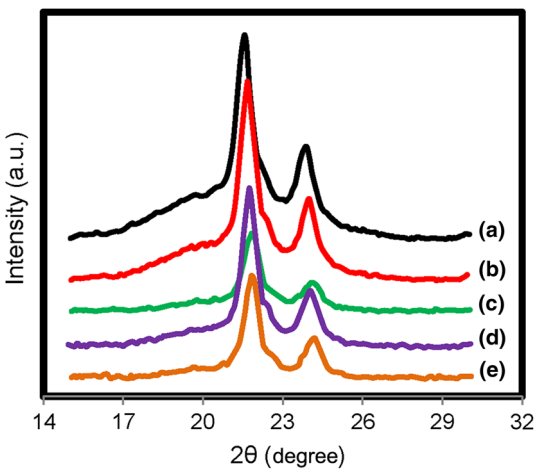

Fig. 5 WAXD patterns of: **a** 4000-24, **b** ionomer I, **c** ionomer II, **d** ionomer III, and **e** ionomer IV samples

Crystalline structure

Typical WAXD patterns for all the samples studied are shown in Fig. 5. Two sharp peaks are observed at about 2θ of 21.6° and 23.3°, indicating the crystallization of soft segment chains for all the SMPUs prepared. These two are the characteristic peaks of polycaprolactone diols with the molecular weight of 4000, as reported by Kim et al. [41]. The results showed that in addition to the polycaprolactone diols, which were long enough to crystallize, the existence of symmetric MDI contributed to the formation of crystalline regions. Moreover, this is in agreement with the fact that the existence of long-chain polyols caused more phase separation and better soft segment crystallization [42]. This result is also consistent with the melting peaks observed in Fig. 3, revealing that all the synthesized SMPUs have been already crystalline.

Mechanical and shape memory properties

Figure 6a–e shows three thermomechanical cycles for samples with different contents of ionic groups. The difference between the first and second cycle in each sample could be attributed to the disentanglement of the chains during elongation, which was irreversible [43]. The introduction of ionic groups led to more crystalline structures

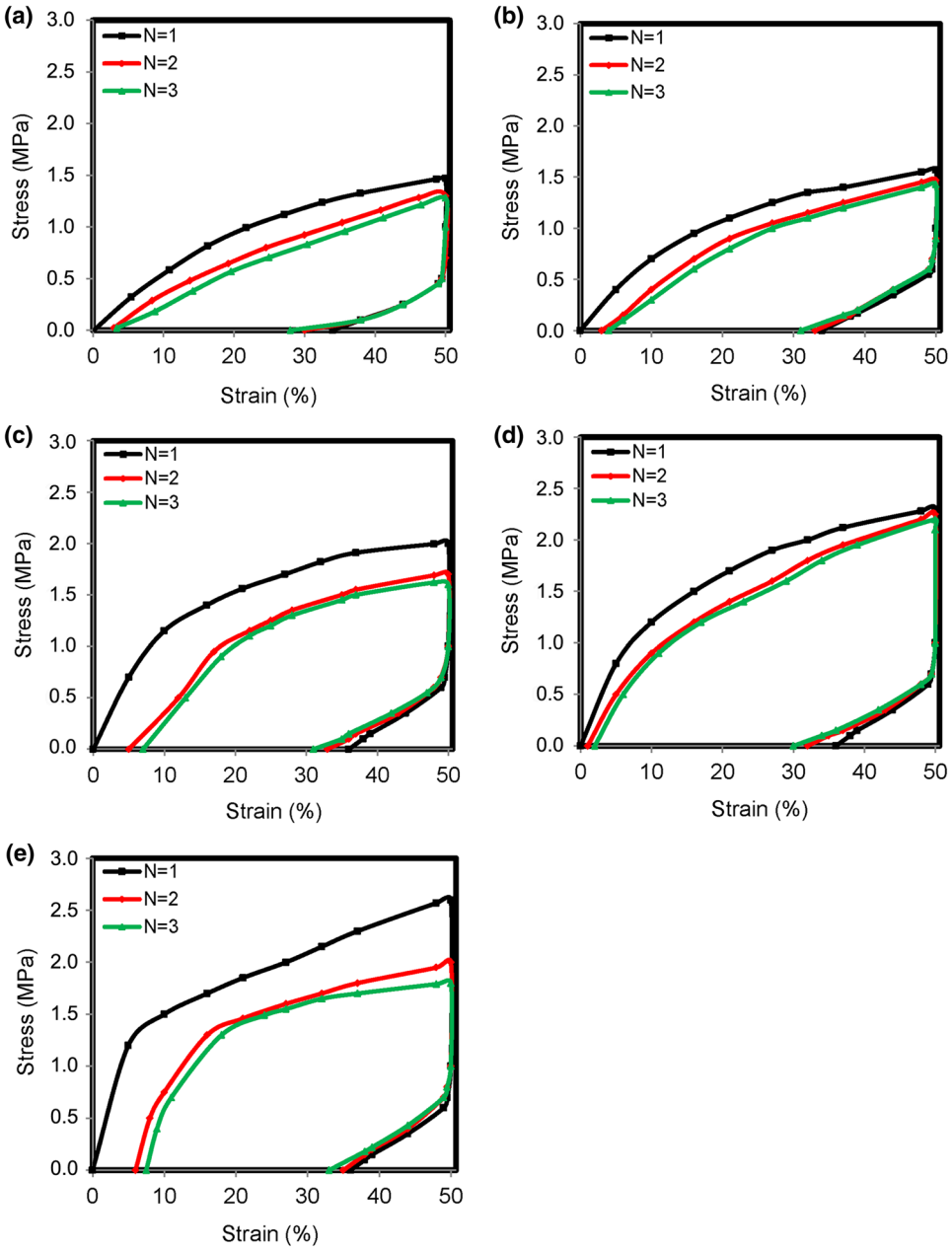

Fig. 6 Thermomechanical cyclic tensile tests of: **a** 4000-24, **b** ionomer I, **c** ionomer II, **d** ionomer III, and **e** ionomer IV samples

Table 4 Maximum tensile stress at the first cycle and shape memory properties of the samples for 50 % elongation after three cycles

Sample name	HSC (%)	Shape fixity R_f (%)	Shape recovery R_r (%)	Maximum tensile stress at the first cycle (MPa)
4000-24	24	69.4 ± 1.2	91.6 ± 1.1	1.47 ± 0.08
Ionomer I	24	71.1 ± 0.9	92.5 ± 0.9	1.57 ± 0.08
Ionomer II	24	70.5 ± 1.3	94.0 ± 1.2	2.00 ± 0.10
Ionomer III	24	74.0 ± 0.8	96.1 ± 0.9	2.30 ± 0.09
Ionomer IV	24	72.0 ± 1.0	97.7 ± 1.1	2.60 ± 0.09

in comparison with non-ionomer sample. Ionic moieties decreased the overall elasticity of the samples, which could be due to the formation of ionic frameworks that prevent easy deformation of polyurethanes. In addition, it was observed that the maximum tensile stress increased, from 1.47 for sample 4000-24 to 2.60 MPa for sample ionomer IV, with the increase of ionic group content. This could be related to the formation of a pseudo-network structure due to the presence of Columbic forces [18, 32].

The values of shape fixity, shape recovery, and maximum tensile stress at the first cycle are given in Table 4. As mentioned before, shape fixation is the ability of a sample to preserve its temporary shape and is dominated by soft segment crystallinity. The maximum shape fixity was observed for ionomer III. However, it could be seen that ionic group content had a few percent influence on shape fixity and shape recovery of the specimens. The improvement of shape recovery could be attributed to the increase of Columbic forces between the hard domains and that of shape fixity to the formation of physical crosslinks, as well as hydrogen bondings between the polymeric chains. Conclusively, the maximum tensile stress was increased with the increase of ionic groups, implying the fact that ionomers showed superior mechanical properties. It was also observed that the shape recovery of the samples was improved with the increase of ionic group content.

Conclusion

A series of polyurethanes were synthesized using PCL-diol, MDI, 1,4-BDO, DMPA, and TEA by bulk polymerization method. FTIR spectrum of all samples showed no characteristic peaks of isocyanate and thus indicated the accomplishment of the synthesis. The data obtained from DSC confirmed a higher degree of crystallinity in ionomers in comparison with non-ionomer sample, implying the fact that the ionic moieties increase the crystallinity of soft segments. The higher degree of crystallization of ionomers was due to the existence of Columbic forces along with hydrogen bonding within the hard segments. WAXD spectra showed that all the samples were crystalline right after the accomplishment of synthesis. Thermogravimetric analysis revealed a lower thermal stability for all the ionomers prepared in comparison with 4000-24 sample. This could be related to the decarboxylation of DMPA and also the formation of more thermodynamically stable molecules, like carbon dioxide and alkenes, as well as the reduction of hydrogen bonds and cohesion in the hard segments of ionomers. Although the shape fixity and shape recovery increased with the increase of ionic group content for a few percent, these improvements were not significant.

Acknowledgments The authors would like to express their appreciation to professor H. Yeganeh for his invaluable comments.

References

1. Huang W (2002) On the selection of shape memory alloys for actuators. Mater Design 23:11–19
2. Hu J, Yang Z, Yeung L, Ji F, Liu Y (2005) Crosslinked polyurethanes with shape memory properties. Polym Int 54:854–859
3. Yang B, Huang WM, Li C, Lee CM, Li L (2004) On the effects of moisture in a polyurethane shape memory polymer. Smart Mater Struct 13:191–195
4. Momtaz M, Razavi-Nouri M, Barikani M (2014) Effect of block ratio and strain amplitude on thermal, structural, and shape memory properties of segmented polycaprolactone-based polyurethanes. J Mater Sci 49:7575–7584
5. Wang CC, Huang WM, Ding Z, Zhao Y, Purnawali H (2012) Cooling-/water-responsive shape memory hybrids. Compos Sci Technol 72:1178–1182
6. Huang WM, Yang B, Zhao Y, Ding Z (2010) Thermo-moisture responsive polyurethane shape-memory polymer and composites: a review. J Mater Chem 20:3367–3381
7. Huang WM, Zhao Y, Wang CC, Ding Z, Purnawali H, Tang C, Zhang JL (2012) Thermo/chemo-responsive shape memory effect in polymers: a sketch of working mechanisms, fundamentals and optimization. J Polym Res 19:9952
8. Chun BC, Cho TK, Chong MH, Chung YC (2007) Structure–property relationship of shape memory polyurethane crosslinked by a polyethylene glycol spacer between polyurethane chains. J Mater Sci 42:9045–9056
9. Sun L, Huang WM, Lu H, Lim KJ, Zhou Y, Wang TX, Gao XY (2014) Heating-responsive shape-memory effect in thermoplastic polyurethanes with low melt-flow index. Macromol Chem Phys 215:2430–2436
10. Barikani M, Zia KM, Bhatti IA, Zuber M, Bhatti HN (2008) Molecular engineering and properties of chitin based shape memory polyurethanes. Carbohydr Polym 74:621–626

11. Zhu Y, Hu J, Yeung LY, Liu Y, Ji F, Yeung KW (2006) Development of shape memory polyurethane fiber with complete shape recoverability. Smart Mater Struct 15:1385–1394
12. Gunes IS, Jimenez GA, Jana SC (2009) Carbonaceous fillers for shape memory actuation of polyurethane composites by resistive heating. Carbon 47:981–997
13. Zia KM, Zuber M, Barikani M, Bhatti IA, Khan MB (2009) Surface characteristics of chitin-based shape memory polyurethane elastomers. Colloid Surface B Biointerfaces 72:248–252
14. Chen S, Hu J, Yuen CW, Chan L (2009) Supramolecular polyurethane networks containing pyridine moieties for shape memory materials. Mater Lett 63:1462–1464
15. Ping P, Wang W, Chen X, Jing X (2007) The influence of hard-segments on two-phase structure and shape memory properties of PCL-based segmented polyurethanes. J Polym Sci Part B Polym Phys 45:557–570
16. Hu JL, Ji FL, Wong YW (2005) Dependency of the shape memory properties of a polyurethane upon thermomechanical cyclic conditions. Polym Int 54:600–605
17. Meng Q, Hu J, Mondal SJ (2008) Thermal sensitive shape recovery and mass transfer properties of polyurethane/modified MWNT composite membranes synthesized via in situ solution pre-polymerization. Membr Sci 319:102–110
18. Matsunaga K, Nakagawa K, Sawai S, Sonoda O, Tajima M, Yoshida Y (2005) Synthesis and characterization of polyurethane anionomers. J Appl Polym Sci 98:2144–2148
19. Tsonos C, Apekis L, Viras K, Stepanenko L, Karabanova L, Sergeeva L (2000) Investigation of the microphase separation in blends of polyurethane-based ionomers. J Macromol Sci Part B 39:155–174
20. Zhu Y, Hu J, Choi KF, Yeung KW, Meng Q, Chen S (2008) Crystallization and melting behavior of the crystalline soft segment in a shape-memory polyurethane ionomer. J Appl Polym Sci 107:599–609
21. Zhu Y, Hu J, Yeung KW, Choi KF, Liu Y, Liem H (2007) Effect of cationic group content on shape memory effect in segmented polyurethane cationomer. J Appl Polym Sci 103:545–556
22. Barikani M, Hepburn C (1987) The relative thermal stability of polyurethane elastomers: 2.Influence of polyol-diisocyanate molar block ratios with a single and mixed diisocyanate system. Cell Polym 6:29–36
23. Ji FL, Hu JL, Li TC, Wong YW (2007) Morphology and shape memory effect of segmented polyurethanes part I: with crystalline reversible phase. Polymer 48:5133–5145
24. Pérez-Limiñana MA, Arán-Aís F, Torró-Palau AM, Orgilés-Barceló AC, Martín-Martínez JM (2005) Characterization of waterborne polyurethane adhesives containing different amounts of ionic groups. Int J Adhes Adhes 25:507–517
25. Tanzi MC, Mantovani D, Petrini P, Guidoin R, Laroche G (1997) Chemical stability of polyether urethanes versus polycarbonate urethanes. J Biomed Mater Res 36:550–559
26. ValipourEbrahimi M, Barikani M, SeyedMohaghegh SM (2006) Synthesis and properties of ionic polyurethane dispersions: influence of polyol molecular weight. Iran Polym J 15:323–330
27. Najafi F, Manouchehri F, Shaabanzadeh M (2011) Synthesis and characterization of anionic polyester-polyurethane dispersion as environmentally-friendly water based resins. J Chem Health Risks 1:23–26
28. Negim SM, Bekbayeva L, Mun GA, Abilov ZA, Saleh MI (2011) Effects of NCO/OH ratios on physico-mechanical properties of polyurethane dispersion. World Appl Sci J 14:402–407
29. Hasing ML, Chang CH, Chan MH, Chao DY (2005) A Study of polyurethane ionomer dispersant. J Appl Polym Sci 96:103–111
30. Chwang CP, Wang CL, Kuo YM, Lee SN, Chao A, Chao DY (2002) On the study of polyurethane ionomer-Part I. Polym Adv Technol 13:285–292
31. Seidel A (2008) Characterization and analysis of polymers. Wiley, Hoboken
32. Kim BK, Lee YM (1992) Structure-property relationship of polyurethane ionomer. Colloid Polym Sci 270:956–961
33. Król P (2007) Synthesis methods, chemical structures and phase structures of linear polyurethanes. Properties and applications of linear polyurethanes in polyurethane elastomers, copolymers and ionomers. Prog Mater Sci 52:915–1015
34. Hourston DJ, Williams GD, Satguru R, Padget JC, Pears D (1999) The influence of the degree of neutralization, the ionic moiety, and the counterion on water-dispersible polyurethanes. J Appl Polym Sci 74:556–566
35. Skarja GA, Woodhouse KA (2001) In vitro degradation and erosion of degradable, segmented polyurethanes containing an amino acid-based chain extender. J Biomater Sci Polym Ed 12:851–873
36. Fukushima K, Tabuani D, Camino G (2009) Nanocomposites of PLA and PCL based on montmorillonite and sepiolite. Mater Sci Eng 29:1433–1441
37. Kim BK, Lee JC (1996) Polyurethane ionomer dispersions from poly (neopentylene phthalate) glycol and isophoronediisocyanate. Polymer 37:469–475
38. Grasel TG, Cooper SL (1989) Properties and biological interactions of polyurethane anionomers: effect of sulfonate incorporation. J Biomed Mater Res 23:311–338
39. Asif A, Shi W, Shen X, Nie K (2005) Physical and thermal properties of UV curable waterborne polyurethane dispersions incorporating hyper branched aliphatic polyester of varying generation number. Polymer 46:11066–11078
40. Lu MG, Lee JY, Shim MJ, Kim SW (2002) Thermal degradation of film cast from aqueouspolyurethane dispersions. J Appl Polym Sci 85:2552–2558
41. Kim BK, Lee SY (1996) Polyurethanes having shape memory effects. Polymer 37:5781–5793
42. Subramani S, Lee JM, Cheong IW, Kim JH (2005) Synthesis and characterization of water-borne cross-linkedsilylated polyurethane dispersions. J Appl Polym Sci 98:620–631
43. Meng Q, Hu J, Zhu Y, Lu J, Liu Y (2007) Polycaprolactone-based shape memory segmented polyurethane fiber. J Appl Polym Sci 106:2515–2523